Tursina et al. *IJDM (2023) 6:3, pp 275-288*
DOI: https://doi.org/10.24815/ijdm.v6i2.34538

International Journal of Disaster Management
E-ISSN: 2527-4341 P-ISSN: 2808-439X

RESEARCH ARTICLE Open Access

Influence of Tides Level on Tsunami Hydrodynamic in Banda Aceh, Indonesia

Tursina Tursina[1,4,5], Syamsidik Syamsidik[1,2,4,*], Shigeru Kato[1,3], and Mochammad Afifuddin[1,2]

[1] Doctoral Program, School of Engineering, Post Graduate Program, Universitas Syiah Kuala, Banda Aceh, 23111 Indonesia.
[2] Civil Engineering Department, Faculty of Engineering, Universitas Syiah Kuala, Banda Aceh, 23111 Indonesia.
[3] Department of Architecture and Civil Engineering, Toyohashi University of Technology, Toyohashi, Aichi 441-8580, Japan.
[4] Tsunami and Disaster Mitigation Research Center (TDMRC), Universitas Syiah Kuala, Banda Aceh, 23111 Indonesia.
[5] Civil Engineering Department, Politeknik Negeri Lhokseumawe, Lhokseumawe, 24301, Indonesia.
***Corresponding author:** syamsidik@usk.ac.id

Received 2 October 2023; *Received in Revised Form* 29 December 2023; *Accepted* 15 January 2024

Abstract

Tides are the dominant physical process in the coastal environment. During high tide, water from the ocean flows through the bays and estuaries, causing inundation and raising water elevation. When low tides condition, the water level becomes lower than average and recedes into the sea. This process continues for a long day. Tsunami waves will interact with all coastal processes and affect the hydrodynamic forces of tsunami waves. In the deep sea, tides do not significantly influence wave propagation. However, in the shallow water zone, tides can change tsunami heights and affect the extent of inundation. Tides are usually ignored in tsunami hazard analysis. This would be an underestimate of the tsunami hazard calculation. This study aims to investigate tides' influence on tsunami runup hydrodynamics in Banda Aceh. The potential tsunami from an earthquake in the Aceh-Andaman subduction zone is modeled using COMCOT (Cornell Multi Grid Coupled Tsunami Model) with magnitudes Mw 9.2, 8.6, and 8.2. We simulated the response of the three earthquake magnitudes on two different types of high and low tides. Several virtual gauges were placed to observe the tsunami height. Virtual gauges were also used to observe the tsunami arrival time at four tsunami escape buildings in Banda Aceh: the Ulee Lheue escape building, the Deah Glumpang escape building, the Alue Deah Teungoh escape building, and the Lambung escape building. The results show that the highest tide amplifies the tsunami inundation will be extended to about 30% farther inland compared to the condition if the tsunami occur during mean sea level condition. The interactions between tsunami and high tide significantly shorten tsunami arrival time on small magnitude tsunamis and are not significant in a large tsunami. This information is useful for enhancing early warning systems and evacuation procedures that can be adjusted to the tidal conditions in the study area.

Keywords: tsunami-tide interaction; escape building; tsunami maximum; tsunami arrival time; numerical simulation.

Introduction

Tsunami waves interact with all physical ocean processes such as tides, currents, wind- and storm-driven waves, water movement in estuaries, and other coastal hydrodynamic processes. Tides are the most dominant physical process in coastal environments. Tsunami waves and tidal waves are both long waves (Dean & Dalrymple, 1991). However, they are different and occur due to unrelated natural phenomena. In the deep sea, tsunamis do not influence by tides due to the relatively small wave height and deep sea depth. However, the interaction of tsunamis with tides in the shallow sea significantly affects the height of the tsunami (Gao & Niu, 2022). Theoretically, changes in sea depth will affect the speed and magnitude of tsunami waves in shallow areas (Kowalik & Proshutinsky, 2010). Previously, tides tended to ignore in tsunami mitigation calculations. Ignoring tide can reduce the accuracy of estimates for tsunami disaster mitigation planning. Recently, many studies have shown the influence of tides on tsunamis. Studies on the coupling of tsunami waves and tides have been conducted in several cases and gained new insights. They also strongly recommend including tides' effects in the tsunami analysis study.

Mofjeld et al. (Mofjeld et al., 2007) proved that tides affect tsunami heights in the Pacific Sea. Other studies investigated the impact of tsunamis and tides in river estuaries (Zhang et al., 2011); (Shelby et al., 2016) and Canal (Winckler et al., 2017), which caused the final wave run-up and inundation to be larger. The research results by Ayca et al. (Ayca et al., 2017) showed that tsunami and tidal interaction can cause maximum current inside Port and Harbor. Some studies focus on tsunami-induced wave propagation with tides (Lehfeldt et al., 2007);(Lee et al., 2015). Coupled modeling of the tsunami and astronomical tide was also conducted in the East China Sea, finding the wave propagation speed to be faster and the propagation time to be shorter (L. Wang & Ying, 2018). The results of Gao et al.'s study (Gao & Niu, 2022) in the nearshore area explained that high tides cause the tsunami height to increase. From these studies, it is known that the role of tides in influencing the hydrodynamics of tsunami waves is significant and, therefore, important to consider in assessing the threat of future tsunamis.

The hydrodynamic characteristics of tsunami waves, in this case, the height and speed of the waves, will affect the arrival time of the tsunami. By knowing the tsunami arrival time, early warning planning for evacuation can be carried out. After the 2004 tsunami, Banda Aceh built 4 Escape Buildings that functioned as temporary shelters for evacuation during a tsunami (Yuzal et al., 2017). This study aims to investigate the influence of tides on tsunami hydrodynamics conditions (flow depth), and this further is used to determine the tsunami arrival time at the four escape buildings in Banda Aceh. This research was conducted with a numerical experiment to see the influence of tides on the tsunami arrival time at the Escape Building.

Study Area

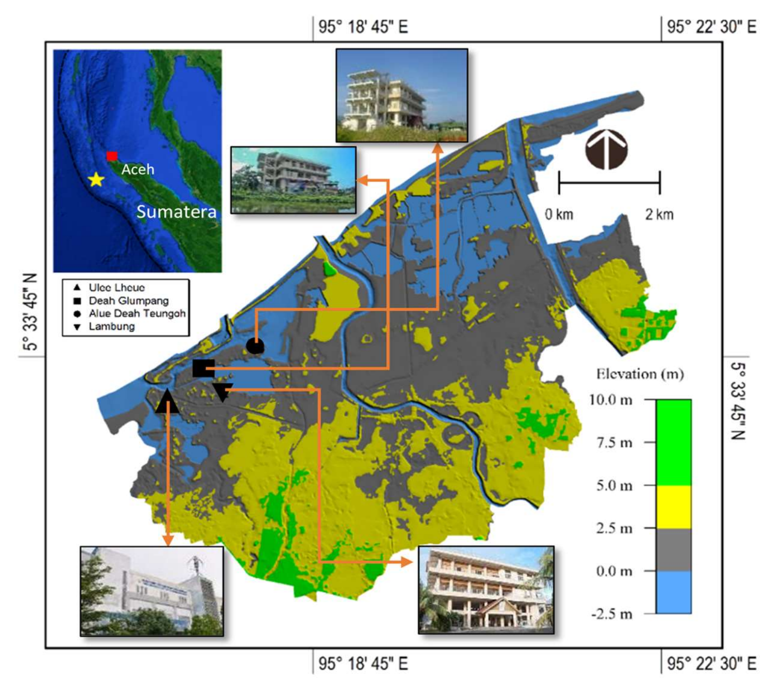

Figure 1. The study area. The map represents the map elevation and the location of the Escape Building in Banda Aceh: Escape Building Ulee Lheue, Deah Glumpang, Alue Deah Teungoh, and Lambung. The map is overlayed on DEM data.

The city of Banda Aceh, which is located in the northern part of Sumatra Island, does not directly face a subduction zone like the west coast of Aceh. Tsunami waves from this source first reached the west coast of Aceh and then arrived in Banda Aceh. Based on studies of tsunami arrival times on the west coast, for example, in Calang, the tsunami arrived 29 minutes after the earthquake. In comparison, in Banda Aceh, the tsunami arrived 35 minutes after the earthquake (Syamsidik et al., 2015). Even so, the tsunami's impact was more significant in Banda Aceh because the dense population and relatively flat topography made it easier for tsunami waves to run up without obstacles. Fig. 1 is a topographic map of Banda Aceh. Elevations below 2.5 m dominate land height. Land elevations above 2.5 m are found in the southern part of the city. In Banda Aceh, areas with ground elevation higher than 5 m are limited and they are located far to the inland ward direction. Therefore, the absence of such higher ground areas requires the city to construct tsunami evacuation buildings to facilitate the tsunami evacuees. There are 4 single purpose escape buildings in Banda Aceh (Jihad et al., 2023): Ulee Lheue, Deah Glumpang, Alue Deah Tengoh, and Lambung Escape Building. All four buildings are located in the Meuraxa sub-district. Fig. 1 also shows the location of escape buildings in Banda Aceh.

Methods

Tsunami Hydrodinamic Model

This research was performed using a numerical simulation method. The hydrodynamic model used for numerical simulation is COMCOT (Cornell Multi Grid Coupled Tsunami). COMCOT has been widely used for tsunami hazard assessment globally. COMCOT requires earthquake parameter data and information on sea depth and bathymetry to generate tsunami waves. This study uses earthquake sources from Sumatra-Andaman. The tsunami wave generation earthquake was modeled with 3 earthquake magnitudes. The 9.2 Mw earthquake was proposed by Koshimura et al. (Koshimura et al., 2009). The Well and Coppersmith equations were used to estimate the rupture dimension for moderate and small magnitudes, namely 8.6 Mw and 8.2 Mw (Wells & Coppersmith, 1994). Detailed characteristics and dimensions of the rupture area due to the simulated earthquakes can be seen in Table 1.

Table 1. The fault parameters for designed tsunami source in the Sumatera-Andaman Subduction Zone.

Fault Parameter	8.2 Mw (single fault)	8.6 Mw (multi fault)		9.2 Mw (multi fault)					
	1	1	2	1	2	3	4	5	6
Epicenter, Lon (°)	94.162	93.32	92.87	94.4	93.32	92.87	92.34	91.88	91.9
Epicenter, Lat (°)	5.67	4.48	5.51	3.03	4.48	5.51	7.14	8.47	11.0
Length of Fault Plane (km)	216.77	125	180	200	125	180	145	125	380
Width of Fault Plane (km)	56.49	80	80	150	150	150	150	150	150
Focal Depth (km)	10	10	10	10	10	10	10	10	10
Dislocation (m)	5.9	9.4	9.4	14	12.6	15.1	7	7	7
Strike direction (°)	329	335	340	323	335	340	340	345	7
Dip angle (°)	8	15	15	15	15	15	15	15	15
Rake (slip) angle (°)	110	90	90	90	90	90	90	90	90

The mathematical equations used to generate tsunami waves were the NSWE and SWE equations shown below. Detailed information on the theoretical background and validation of COMCOT can be found in Wang and Liu (X. Wang & Liu, 2006).

$$\frac{\partial \eta}{\partial t} + \frac{1}{R\cos\varphi}\left\{\frac{\partial P}{\partial \varphi} + \frac{\partial}{\partial \varphi}(\cos\varphi Q)\right\} = 0, \qquad (1)'$$

$$\frac{\partial P}{\partial t} + \frac{gh}{R\cos\varphi}\frac{\partial \eta}{\partial \psi} - fQ = 0, \qquad (2)'$$

$$\frac{\partial Q}{\partial t}+\frac{gh}{R}\frac{\partial \eta}{\partial \varphi}+fP=0, \quad (3)'$$

The nonlinear SWEs are explained in Eq. (4) – (10) as follows:

$$\frac{\partial \eta}{\partial t}+\frac{1}{R\cos\varphi}\left\{\frac{\partial P}{\partial \psi}+\frac{\partial}{\partial \varphi}\cos\varphi\, Q\right\}=0, \quad (4)'$$

$$\frac{\partial P}{\partial t}+\frac{1}{R\cos\varphi}\frac{\partial}{\partial \psi}\left\{\frac{P^2}{H}\right\}+\frac{1}{R}\frac{\partial}{\partial \varphi}\left\{\frac{PQ}{H}\right\}+\frac{gH}{R\cos\varphi}\frac{\partial \eta}{\partial \psi}-fQ+F_x=0, \quad (5)'$$

$$\frac{\partial Q}{\partial t}+\frac{1}{R\cos\varphi}\frac{\partial}{\partial \psi}\left\{\frac{PQ}{H}\right\}+\frac{1}{R}\frac{\partial}{\partial \varphi}\left\{\frac{Q^2}{H}\right\}+\frac{gH}{R}\frac{\partial \eta}{\partial \varphi}+fP+F_y=0, \quad (6)'$$

$$f=\Omega\sin\varphi, \quad (7)'$$

Where η is the elevation of water's surface; (*P*, *Q*) stand for the volume fluxes in *X* (West-East) and *Y* (South-North) direction, respectively; (φ, ψ) denotes the latitude and longitude of the Earth; *R* for radius; *g* for its acceleration due to gravity and *h* is the water depth; *f* is symbolized the Coriolis force. *H* is the total water depth; and *n* represents Manning's roughness coefficient.

Manning's formulas are explained as follows:

$$F_y=\frac{gn^2}{H^{7/3}}P(+Q^2)^{1/2}, \quad (8)'$$

$$F_y=\frac{gn^2}{H^{7/3}}Q(P^2+Q^2)^{1/2}, \quad (9)'$$

$$\mathrm{H}=\eta+\mathrm{h}, \quad (10)'$$

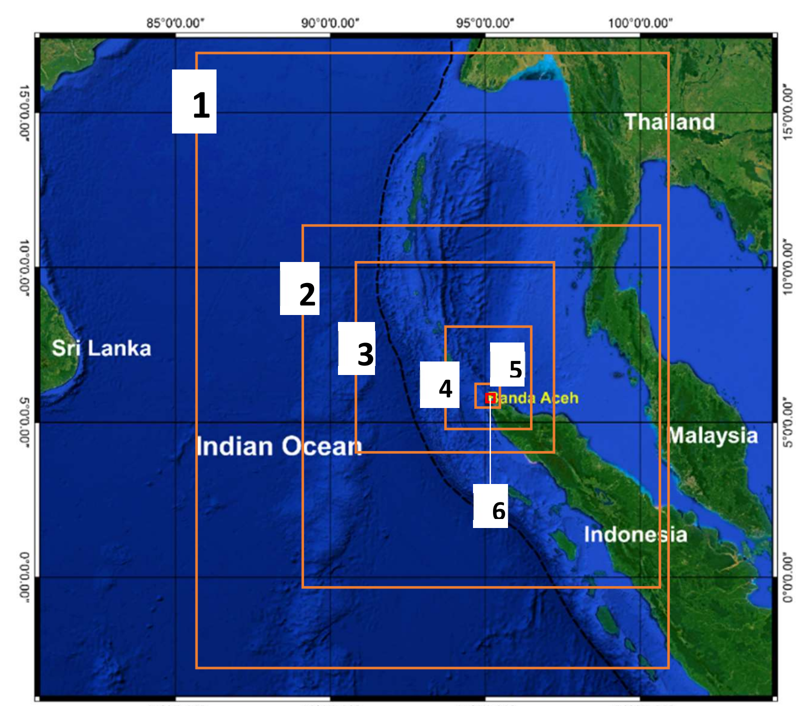

Figure 2. The layout of computational grid for tsunami numerical simulation.

The research utilized a system of six nested grids, as illustrated in Fig 2. The purpose of using a nested grid is to reduce computation simulation time and obtain detailed grid resolution in the study area. The Layer 1 was aimed to simulate the initial tsunami propagation from its source and propagated around the Indian Ocean basin, with a resolution of 1 arc-min (approximately 1856 m). This grid was created using data from the 30 arc-min General Bathymetric Chart of the Oceans (GEBCO). The Layers 2, 3, and 4 of the simulation domain were derived from Layer 1 with their grids the resolutions are 928 m, 309 m, and 103 m, respectively. The Layers 3 and 4 covered the Aceh Province. Layer 5 of the simulation covered Aceh Besar and Banda Aceh with their resolutions were three times smaller than grid size in Layer 4 (34 m). The finest grid is at Layer 6 with its grid size was 8.6 m. The finest grid level was built from bathymetry data provided by Indonesia National Bathymetry (BATNAS) and nearshore bathymetry were surveyed by Tsunami and Disaster Mitigation Research Center (TDMRC) in 2017. High resolution of topography was adopted from Japan International Cooperation Agency (JICA).

In this research, bottom frictions were characterized by applying a Manning's roughness coefficient, with spatial variation according to difference land uses/covers on 2004, before the tsunami. We classified the study area into six types of landuses as recommended by (Syamsidik et al., 2017). This was done through digitizing aerial images of the targeted area taken in June 2004 (before the tsunami). Land uses/cover types and Manning's coefficient used are: water (0.013), bare land (0.02), built-up area (0.04), ponds (0.017), and vegetation (0.035) as recomended by (Li et al., 2012). The values were chosen based on the guide for selecting Manning's coefficients for natural channels and floodplains (Arcement & Schneider, 1989). Manning's roughness was applied in Layer 6 where tsunami inundation and tsunami time of arrival were observed.

The numerical simulation's validation was performed using parameters *K* and *k*, as define by Eqs. (11) and (12) (Aida, 1978).

$$\log K = \frac{1}{n}\sum_{i=1}^{n} \log K_i \quad (11)'$$

$$\log \kappa = \sqrt{\frac{1}{n}\sum_{i=1}^{n}(\log K_i)^2 - (\log K)^2} \quad (12)'$$

$$K_i = \frac{h_{obs-i}}{h_{sim-i}} \quad (13)'$$

Where h_{obs-i} represents the observed depth of the tsunami flow at location i and h_{sim-i} represents the simulated tsunami flow depth at the same location. The model results will be good agreement if K is in the range of $0.8 \leq K < 1.2$ and $\kappa \leq 1.60$ (Aida, 1978).

Tidal Level in Banda Aceh

Tides significantly affect Banda Aceh's coastal areas. Banda Aceh has a border length of 60 km. A quarter of this border is directly adjacent to the Andaman Sea, with a coastline length of 15 km. Along the coastline, Banda Aceh features two primary river estuary outlets, as well as smaller outlets for fishing boats. During low tide, fishing boats may encounter difficulties navigating these channels, requiring fishermen to wait for the tide to enable entry or exit. Additionally, Banda Aceh has large water bodies, including lagoons and ponds (Meilianda et al., 2019). The Highest High Water Level (HHWL) is 0.86 m, and the Lowest Low Water Level (LLWL) is -0.79 m from the Mean Sea Level (MSL). During certain conditions, such as a supermoon, the tide range can be higher than usual (Flick, 2016); (Banno & Kuriyama, 2020). In this research, tides levels were taken from a series of measurements conducted by TDMRC in 2015 around the river mouth of the Ulee Lheue estuary. The 15-day tides data are shown in Fig. 3.

ISSN: 2527-4341 P-ISSN: 2808-439X, Vol. 6:3, pp 313-326

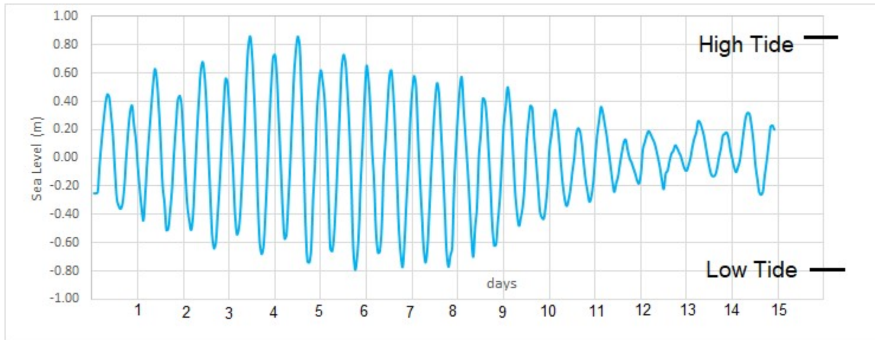

Figure 3. Tidal phase in Banda aceh from field measurement on 2015.

To investigate the impact of tides on tsunami waves, affecting the arrival time, observations were conducted at the escape building location. A total of nine simulations were performed as described in Fig. 4. Tidal data were integrated into the COMCOT model by adding tidal values to the initial water level. A value of 0.0 m represents tsunami-only cases (Tsunami Only). A value of 0.86 m is used to observe the tsunami's impact during high tide conditions (Tsunami + High Tide), while a value of -0.79 m examines the influence of the tsunami during low tide conditions (Tsunami + Low Tide). Tsunami arrival time is determined based on the arrival phase of the first tsunami wave (Benazir et al., 2022). The ETA was indicated when the tsunami wave reaches 0.5 m from its initial level. It is interpreted as a moment when a potentially tsunami hazards start to take place. BMKG (Indonesia's Meteorology, Climatology, and Geophysics Agency) will issue a "Advisory" alert for the implementation of precautionary measures for coastal communities (BKMG, 2012).

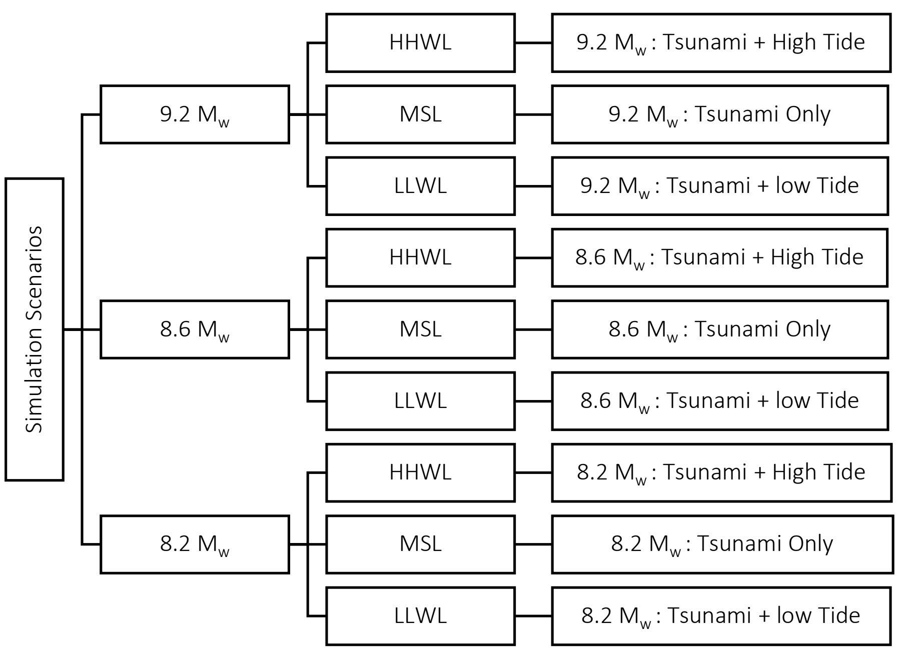

Figure 4. Tsunami simulation scenarios.

Result and Discussion

Changes in Sea Surface Elevation Around Earthquake Zones

The source of tsunami waves in this research was generated from earthquakes in subduction zones of the Aceh-Andaman segment. The sea level is disturbed when an underwater fault occurs that causes an earthquake. Fig.5a shows the initial sea level conditions during the 2004 earthquake and tsunami. The source of the fault was located from the southern part of Aceh to Andaman Island (Aceh-Andaman Segment) (Sieh, 2005); (Koshimura et al., 2009); (Meltzner et al., 2010); (Jihad et al., 2020). The modeling results show that the water level decreased or receded shortly after the earthquake on the west coast of Aceh. Fig. 5b. and Fig. 5c. show the modeling of moderate earthquakes with magnitudes of 8.6 Mw and 8.2 Mw that produced initial surface elevation at the source and could have potentially propagated the tsunami to Banda Aceh.

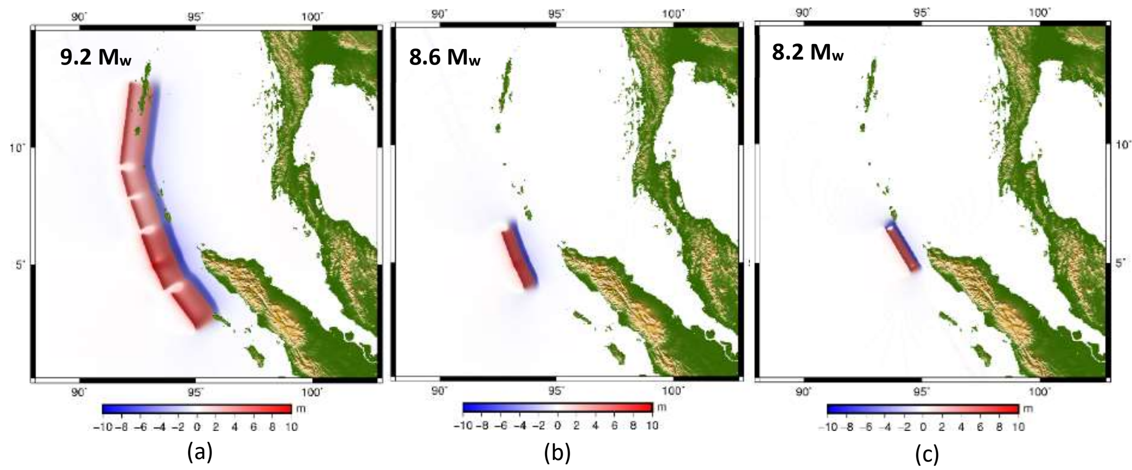

Figure 5. Initial sea surface conditions following earthquakes with magnitudes (a) 9.2 Mw, (b) 8.6 Mw, and (c) 8.2 Mw around the ruptured area. The red color indicates the sea level is rising, and the light blue indicates the water level is falling.

Model Validation

The 2004 tsunami had an impact on the tsunami inundation in the study area of Banda Aceh. Several post-tsunami surveys were conducted to measure the tsunami heights, recorded through tsunami poles (Iemura et al., 2012). This dataset were used as a benchmark for validating the parameters of the tsunami simulation model using the Aida equation (Aida, 1978). The validation process has been comprehensively performed in previous research and it indicated a strong correlation between the simulated tsunami height and the observed results. A more detailed report on this can be referred to the studies (Tursina & Syamsidik, 2019) and (Tursina et al., 2021). The validation was also conducted by creating inundation maps, comparing the simulated tsunami inundation boundaries with those obtained from satellite image interpretation. The validation results show that the simulation model adequately represents the extent of the tsunami inundation. Furthermore, the comparison results reveal that the 2004 tsunami occurred under normal sea level conditions. The validation of tsunami inundation between simulation results and field measurement can be seen in Fig. 6.

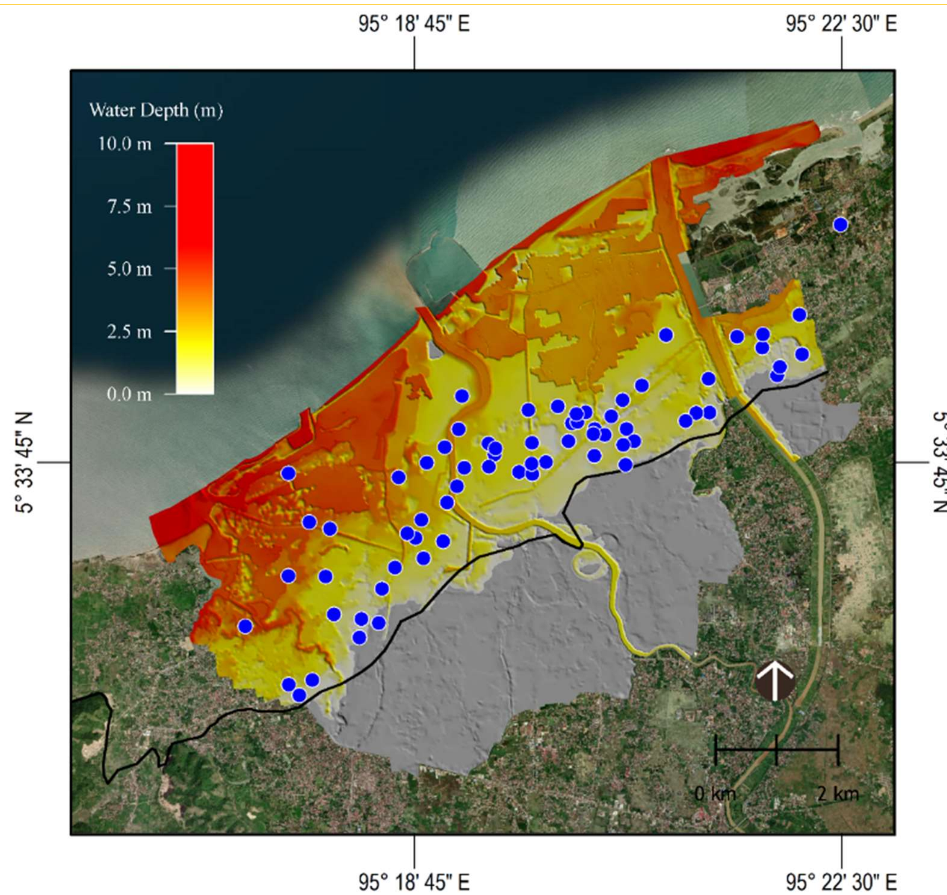

Figure 6. The validation of a tsunami numerical model conducted based on water depth and the inundation area. The colored map overlaid on world imagery is the maximum tsunami map resulting from the simulation. The black line denotes the boundary of the 2004 tsunami inundation. The blue point marks the location of the tsunami pole, indicating the watermark of the 2004 tsunami.

Influence of Tides on Tsunamis

To see the influence of tides on tsunamis, simulations with and without tides were conducted. Fig. 7 illustrates the time series results of tsunami heights and arrival times at each escape building. Fig. 6a shows the arrival time of the tsunami caused by the 9.2 Mw earthquake from three simulations: high tide, low tide, and tsunami only. In each line plot on the graph, the tsunami height with high tide shows the most significant results with an amplification range of 0.5 – 1.0 m. The lowest tsunami height is found at low tide, and the moderate tsunami observes at the tsunami only without tide. This indicates that the tsunami wave height is enhanced by the high tide's interaction and declined by the low tide. The wave pattern shows the same trend in all four escape buildings.

The arrival time of the tsunami at the escape building can also be observed in Fig. 7a. Tsunami waves caused by an earthquake of Mw 9.2 will arrive at the escape building in Banda Aceh about 40 minutes after the earthquake. The arrival time of the first wave is approximately the same at all four escape buildings. The simulation results found that high and low tides caused the arrival time of tsunami waves to be faster or slower by an average of 0.5 - 1.0 minutes compared to tsunami waves alone. Tsunami waves arrive faster at the escape buildings during high tide conditions and slower during low tide. The simulation results of Case Mw 9.2 found that adding tides does not significantly affect the tsunami arrival time at the escape building. This implies that in the worst-case scenario (the most significant earthquake), the tsunami wave itself is more dominant so that the tides do not significant affect the arrival time of the tsunami on the run-up area.

The tsunami height was also calculated at an earthquake magnitude of 8.6 Mw (Fig. 7b). The interaction of tides with tsunamis also showed the same tendency, with the highest tide impacting the tsunami height relatively more. The tidal impact was observed during the first wave at the Alue Deah Tengoh escape building. At this building, the tsunami height became 2 m due to the interaction with the tide. The tsunami arrival time at the escape building was 51 minutes after the earthquake. At high tide, the arrival time accelerated by about 2 minutes and slowed by 2 minutes at low tide. Some studies have shown similar results (Gao & Niu, 2022); (Ren et al., 2022) if a tsunami arrives at the coast when a high tidal level, the arrival time of the tsunami is advanced.

Interestingly, more varied results are found at the smaller magnitude of 8.2 Mw (Fig. 7c). The difference in maximum tsunami height is relatively larger with and without tidal interaction. The maximum tsunami height at the Deah Glumpang escape building differs by up to 1 m compared to the tsunami alone. In contrast, the maximum tsunami height at low tide is only 0.2 m. Previous studies have also highlighted that the interaction of the highest tide during a tsunami has been shown to increase the height of the tsunami (Mofjeld et al., 2007); (Lee et al., 2015).

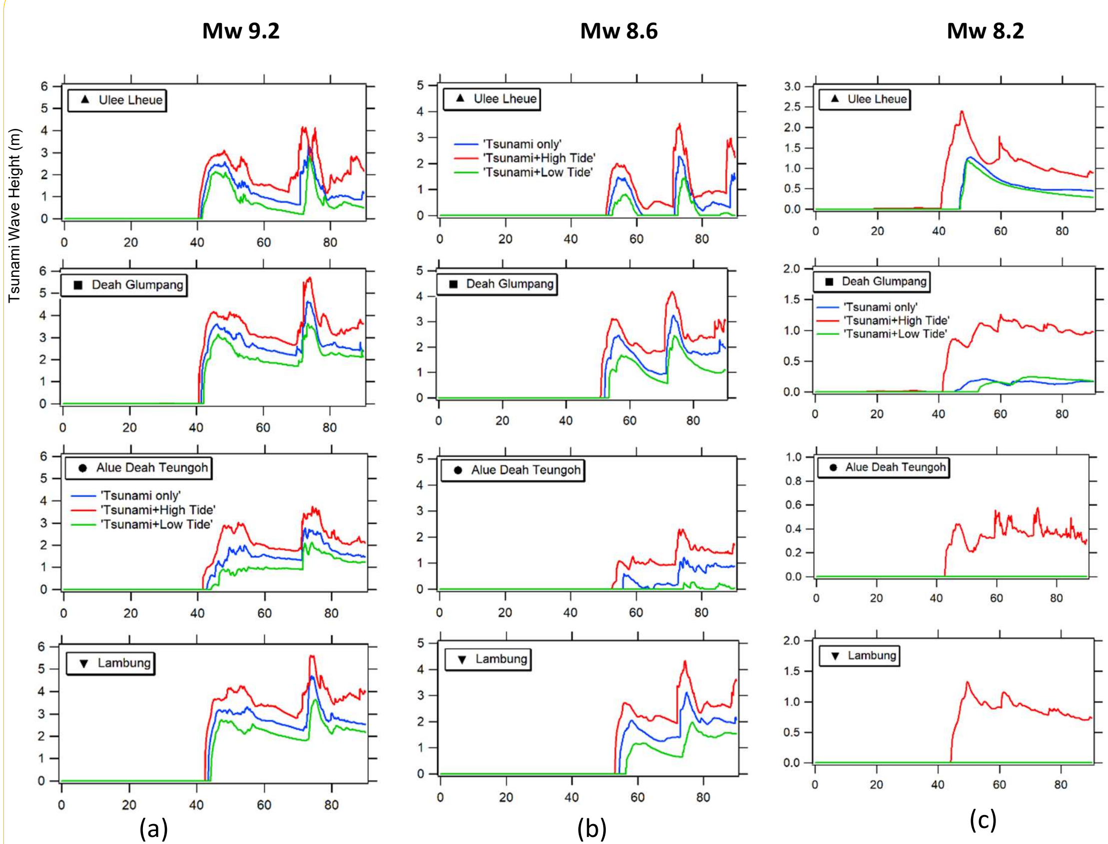

Figure 7. The comparison of simulated tsunami wave height at four tsunami escape buildings: Ulee Lheue, Deah Glumpang, Alue Deah Teungoh and Lambung. Each plot presents the sea level variation from the tsunami without tide (*tsunami only*), the coupled high tide with the tsunami (*tsunami+high tide*) and the tsunami height at low tide (*tsunami+ low tide*). The first tsunami wave at the observation point determines by the tsunami arrival time.

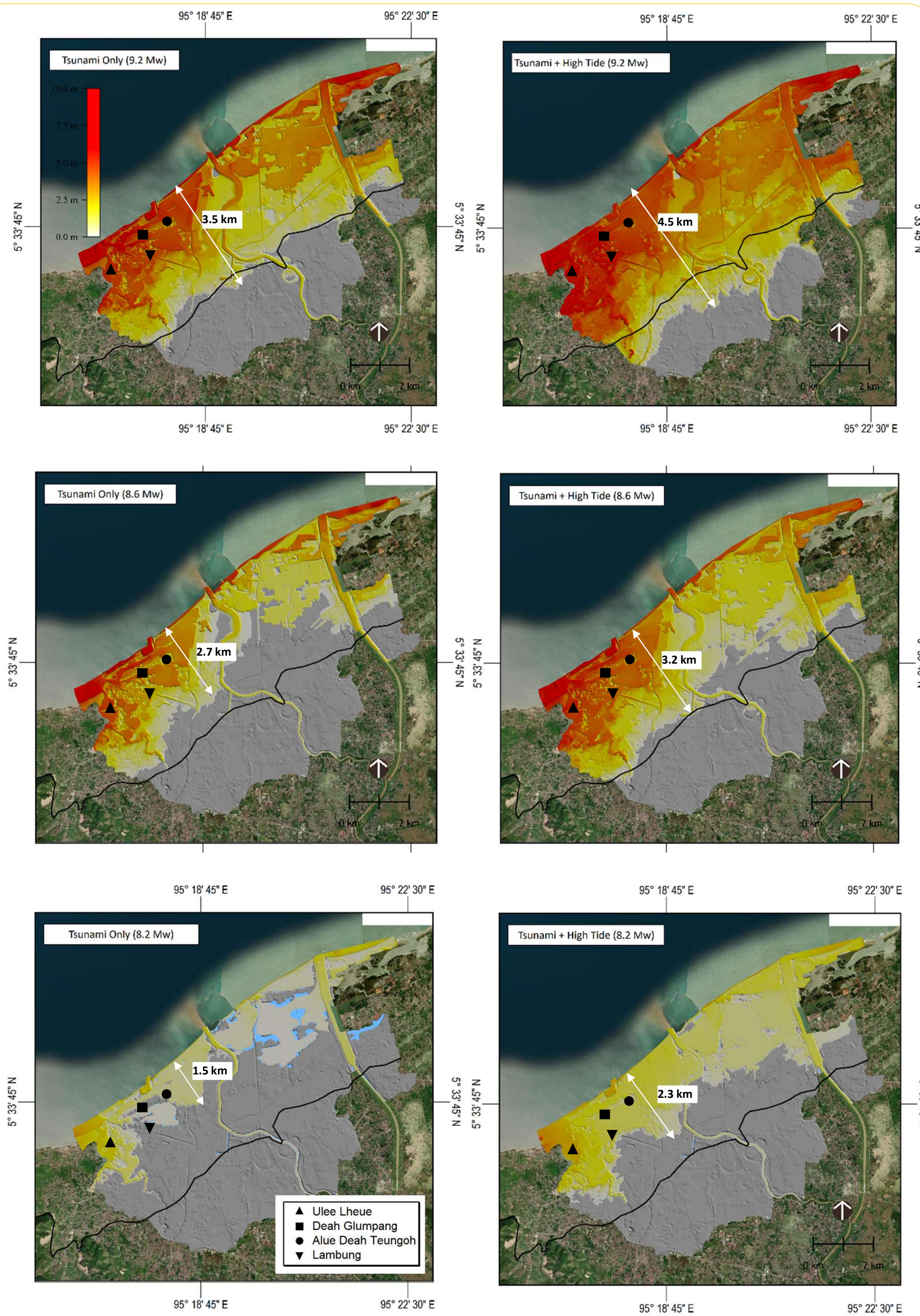

Figure 8. The tsunami inundation maps for tsunami-only scenario compare with a scenario of a tsunami combined with high tides at different magnitudes. Different markers represent the locations of tsunami escape buildings. The solid black line indicates the boundary of the 2004 tsunami inundation.

Regarding the arrival time, at average, the first wave will arrive at the built-up area about 47 minutes after the earthquake. The arrival time would be 7 minutes faster if the tsunami interacted with the tide. The effect of tides clearly shows the tsunami wave could onky reach Alue Deah Teungoh and Lambung escape buildings during high-tides condition. Without tidal influence, the tsunami waves will not reach these escape building locations. These observations highlight the more significant role of tides when tsunamis are generated by smaller earthquakes, such as 8.2 Mw (Fig. 7c).

The effect of tidal interaction with tsunamis was also examined in the tsunami inundation area. Fig. 8 shows the map of maximum inundation in Banda Aceh at different magnitudes with and without the highest tide. The map shows a large difference between the inundation area without tide and tsunami with the highest tide. The inundation area of a tsunami extent will reach 30% farther inlandward area when a tsunami occurs during the highest tide condition compared to the mean sea level condition. Changes in water depth in shallow water due to tides impact the reach of run-up waves to the land. The higher the sea level elevation, the farther the wave run-up will be. Similar results were found by previous studies that the combined tidal wave and tsunami play an important role in the final wave run-up and inundation (Zhang et al., 2011); (Kim et al., 2021); (Gao & Niu, 2022). Moreover, it should also be noted that the response to the tidal-tsunami combination varies depending on the elevation of the topography. Land use/cover also contributes to the degree of severity in tsunamis inundation.

Conclusions

This study uses numerical simulations to investigate the impact of tides on tsunami height and arrival time. The present study is based on the scenario of three earthquakes with magnitudes of Mw 9.2, 8.6 and 8.2 from the Aceh-Andaman fault that can potentially generate a tsunami in Banda Aceh. Based on the results of these numerical simulations, the difference in seawater depth in shallow seas due to tides results in higher tsunami heights at high tides and faster tsunami arrival times in Banda Aceh. Likewise, if the water surface recedes, the tsunami wave height will be lower, and the tsunami arrival time will be longer when compared to a tsunami alone.

The main conclusion of this study is that the tides influence on tsunami arrival time is insignificant if the earthquake magnitude is large because tsunami waves are more dominant. However, tides greatly influence smaller earthquake magnitudes, such as 8.2 Mw. Minor magnitude earthquakes can greatly impact if they occur during the highest tides. From this study, it can be concluded that tides play a major role in the hydrodynamics of tsunami waves. For this reason, it is recommended that tsunami early warnings be based on tidal waves. Ongoing long-term monitoring is required to measure the potential maximum height of local tsunamis.

Acknowledgments

The authors would like to thank Indonesia's Ministry of Education, Culture, Research, and Technology (KEMENDIKBUDRISTEK) under Research Grant *Penelitian Disertasi Doktor* (PDD) year 2022. Research Contract No. 145/E5/PG.02.00.PT/2022.

References

Aida, I. (1978). Reliability of a Tsunami Source Model Derived From Fault Parameters. *J. Phys. Earth*, 57–73.

Arcement, G. J., & Schneider, V. R. (1989). Guide for Selecting Manning ' s Roughness Coefficients for Natural Channels and Flood Plains Guide for Selecting Manning ' s Roughness Coefficients for Natural Channels and Flood Plains. *United States Geological Survey Water-Supply Paper 2339*.

Ayca, A., Lynett, P. J., & Wilson, R. (2017). Effects of Tide and Wave Directionality on Localized Tsunami-Induced Currents in Port and Harbors. *Coastal Engineering Proceedings*, *35*, 8. https://doi.org/10.9753/icce.v35.currents.8

Banno, M., & Kuriyama, Y. (2020). Supermoon Drives Beach Morphological Changes in the Swash Zone. *Geophysical Research Letters*. https://doi.org/10.1029/2020GL089745

Benazir, Kuswandi, Aslami, M. H., Ikhwali, M. F., & Hijah, S. N. (2022). Estimated Tsunami Arrival Time Based on The Aceh-Andaman Fault Segment for North Coast of Aceh. *Jurnal Teknik Hidraulik*, *13*, 65–76.

BKMG. (2012). *Tsunami Early Warning Service Guidebook for InaTEWS*. BMKG.

Dean, R. G., & Dalrymple, R. A. (1991). *Water wave mechanics for engineers and scientists* (P. L. F. Liu (ed.); Issue 2). World Scientific.

Flick, R. E. (2016). California tides, sea level, and waves — Winter 2015-2016. *Shore & Beach*, *84*(2).

Gao, X., & Niu, X. (2022). Influence of tidal level on quantifying the probability of nearshore tsunami hazard. *Ocean Engineering*, *266*(P3), 112986. https://doi.org/10.1016/j.oceaneng.2022.112986

Iemura, H., Pradono, M. H., Sugimoto, M., Takahashi, Y., & Husen, A. (2012). Tsunami Height Memorial Poles in Banda Aceh and Recommendations for Disaster Prevention. *Proceedings of the International Symposium on Engineering Lessons Learned from the 2011 Great East Japan Earthquake*, 1605–1616.

Jihad, A., Muksin, U., Syamsidik, Ramli, M., Banyunegoro, V. H., Simanjuntak, A. V. H., & Rusdin, A. A. (2023). Tsunami evacuation sites in the northern Sumatra (Indonesia) determined based on the updated tsunami numerical simulations. *Progress in Disaster Science*, *18*(September 2022), 1–16. https://doi.org/10.1016/j.pdisas.2023.100286

Jihad, A., Muksin, U., Syamsidik, Suppasri, A., Ramli, M., & Banyunegoro, V. H. (2020). Coastal and settlement typologies-based tsunami modeling along the northern Sumatra seismic gap zone for disaster risk reduction action plans. *International Journal of Disaster Risk Reduction*, *51*(August), 101800. https://doi.org/10.1016/j.ijdrr.2020.101800

Kim, K. O., Jung, K. T., & Ha, T. M. (2021). Development of a Tsunami-tide Interaction Model with Simulation of Tsunami Wave Propagation to Korea Coasts. *Journal of Coastal Research*, 91–95. https://www.jstor.org/stable/48638725

Koshimura, S., Oie, T., Yanagisawa, H., & Imamura, F. (2009). Developing fragility functions for tsunami damage estimation using numerical model and post-tsunami data from banda aceh, Indonesia. *Coastal Engineering Journal*, *51*(3). https://doi.org/10.1142/S0578563409002004

Kowalik, Z., & Proshutinsky, A. (2010). Tsunami – tide interactions : A Cook Inlet case study. *Continental Shelf Research*, *30*(6), 633–642. https://doi.org/10.1016/j.csr.2009.10.004

Lee, H. S., Shimoyama, T., & Popinet, S. (2015). Impacts of tides on tsunami propagation due to potential Nankai Trough earthquakes in the Seto Inland Sea, Japan. *Journal of Geophysical Research : Oceans*, 6865–6883. https://doi.org/10.1002/2015JC010995.Received

Lehfeldt, R., Milbradt, P., Plüss, A., & Schüttrunpf, H. (2007). Propagation of a tsunami-wave in the North Sea. *Kuste*, *72*, 105–123.

Li, L., Qiu, Q., & Huang, Z. (2012). Numerical modeling of the morphological change in Lhok Nga , west Banda Aceh , during the 2004 Indian Ocean tsunami : understanding tsunami deposits using a forward modeling method. *Nat Hazards*, *64*, 1549–1574. https://doi.org/10.1007/s11069-012-0325-z

Meilianda, E., Pradhan, B., Syamsidik, Comfort, L. K., Alfian, D., Juanda, R., Syahreza, S., & Munadi, K. (2019). Assessment of post-tsunami disaster land use / land cover change and potential impact of future sea-level rise to low-lying coastal areas : A case study of Banda Aceh coast of Indonesia. *International Journal of Disaster Risk Reduction*, *41*(October 2018).

Meltzner, A. J., Sieh, K., Chiang, H. W., Shen, C. C., Suwargadi, B. W., Natawidjaja, D. H., Philibosian, B. E., Briggs, R. W., & Galetzka, J. (2010). Coral evidence for earthquake recurrence and an A . D . 1390 – 1455 cluster at the south end of the 2004 Aceh – Andaman rupture. *Journal of Geophysical Research*, *115*, 1–46. https://doi.org/10.1029/2010JB007499

Mofjeld, H. O., González, F. I., Titov, V. V., Venturato, A. J., & Newman, J. C. (2007). Effects of tides on maximum tsunami wave heights: Probability distributions. *Journal of Atmospheric and Oceanic Technology*, *24*(1), 117–123. https://doi.org/10.1175/JTECH1955.1

Ren, Z., Gao, Y., Ji, X., & Hou, J. (2022). Deterministic tsunami hazard assessment and zoning approach using far-field and near-field sources: Study of Cixi County of Zhejiang Province, China. *Ocean Engineering*, *247*. https://doi.org/10.1016/j.oceaneng.2021.110487

Shelby, M., Grilli, S. T., & Grilli, A. R. (2016). Tsunami hazard assessment in the Hudson River Estuary based on dynamic tsunami – tide simulations. *Pure Appl. Geophys.*, *173*, 337–338. https://doi.org/10.1007/s00024-016-1315-y

Sieh, K. (2005). Aceh–Andaman earthquake: What happened and what's next? *Nature*, *434*, 573–574. https://doi.org/10.1038/434573a

Syamsidik, M Rasyif, T., & Kato, S. (2015). International Journal of Disaster Risk Reduction Development of accurate tsunami estimated times of arrival for tsunami-prone cities in Aceh , Indonesia. *International Journal of Disaster Risk Reduction*, *14*, 403–410. https://doi.org/10.1016/j.ijdrr.2015.09.006

Syamsidik, Oktari, R. S., Munadi, K., Arief, S., & Fajri, I. Z. (2017). Changes in coastal land use and the reasons for selecting places to live in Banda Aceh 10 years after the 2004 Indian Ocean tsunami. *Natural Hazards*, *7*. https://doi.org/10.1007/s11069-017-2930-3

Tursina, & Syamsidik. (2019). Reconstruction of the 2004 Tsunami Inundation Map in Banda Aceh Through Numerical Model and Its Validation with Post-Tsunami Survey Data. *IOP Conf. Series: Earth and Environmental Science*, *273*. https://doi.org/10.1088/1755-1315/273/1/012008

Tursina, Syamsidik, Kato, S., & Afifuddin, M. (2021). Coupling sea-level rise with tsunamis: Projected adverse impact of future tsunamis on Banda Aceh city, Indonesia. *International Journal of Disaster Risk Reduction*, *55*(7), 102084. https://doi.org/10.1016/j.ijdrr.2021.102084

Wang, L., & Ying, C. (2018). Research on astronomical tide and tsunami coupled model. *IOP Conference Series: Earth and Environmental Science*, *153*(2). https://doi.org/10.1088/1755-1315/153/2/022018

Wang, X., & Liu, P. L. F. (2006). An analysis of 2004 Sumatra earthquake fault plane mechanisms and Indian Ocean tsunami. *Journal of Hydraulic Research*, *44*(2), 147–154.

Wells, D. L., & Coppersmith, K. J. (1994). New Empirical Relationships among Magnitude , Rupture Length , Rupture Width , Rupture Area , and Surface Displacement. *Bulletin of the Seismological Society of America*, *84*(4), 974–1002.

Winckler, P., Sepúlveda, I., Aron, F., & Contreras-López, M. (2017). How Do Tides and Tsunamis Interact in a Highly Energetic Channel? The Case of Canal Chacao, Chile. *Journal of Geophysical Research: Oceans*, *122*(12), 9605–9624. https://doi.org/10.1002/2017JC012680

Yuzal, H., Kim, K., Pant, P., & Yamashita, E. (2017). Tsunami evacuation buildings and evacuation planning in Banda Aceh, Indonesia. *Journal of Emergency Management*, *15*(1), 49–61. https://doi.org/10.5055/jem.2017.0312

Zhang, Y. J., Witter, R. C., & Priest, G. R. (2011). Tsunami – tide interaction in 1964 Prince William Sound tsunami. *Ocean Modelling*, *40*(3–4), 246–259. https://doi.org/10.1016/j.ocemod.2011.09.005